# Foot Small Muscle Atrophy Is Present Before the Detection of Clinical Neuropathy

ROBERT L. GREENMAN, PHD[1]
LALITA KHAODHIAR, MD[2]
CHRISTINA LIMA, BA[3]
THANH DINH, DPM[3]
JOHN M. GIURINI, DPM[3]
ARISTIDIS VEVES, MD[3]

**OBJECTIVE** — To characterize structural changes and the metabolic profile of foot muscles and correlate them with diabetic neuropathy measurements using phosphorus-31 ($^{31}$P) rapid acquisition with relaxation enhancement (RARE) magnetic resonance imaging (MRI).

**RESEARCH DESIGN AND METHODS** — We studied 12 control subjects, 9 nonneuropathic diabetic patients, and 12 neuropathic diabetic patients using $^{31}$P RARE and proton ($^{1}$H) MRI at 3 Tesla. The ratio of the total cross-sectional area of the foot to that of the muscle tissue was calculated from transaxial $^{1}$H and $^{31}$P images. The average $^{31}$P concentration across the metatarsal head region was measured from the $^{31}$P images.

**RESULTS** — The muscle area−to−total area ratio differed among all three groups (means ± SD): 0.55 ± 0.04 vs. 0.44 ± 0.05 vs. 0.06 ± 0.06 for control, nonneuropathic, and neuropathic subjects, respectively ($P < 0.0001$). The average $^{31}$P concentration also differed among all groups: 27.7 ± 3.8 vs. 21.7 ± 4.8 vs. 7.9 ± 8.8 mmol/l for control, nonneuropathic, and neuropathic subjects ($P < 0.0001$). The muscle area−to−total area ratio strongly correlated with clinical measurements: Neuropathy Disability Score, $r = -0.83$, $P < 0.0001$; vibration perception threshold, $r = -0.79$, $P < 0.0001$; and Semmes-Weinstein monofilaments, $r = -0.87$, $P < 0.0001$.

**CONCLUSIONS** — Small muscle atrophy is present in diabetes before clinical peripheral neuropathy can be detected using standard clinical techniques. The $^{31}$P RARE MRI method evaluates the severity of muscle atrophy, even in the early stages when neuropathy is absent. This technique may prove to be a useful diagnostic tool in identifying early-stage diabetic foot problems.

*Diabetes Care* 28:1425–1430, 2005

Atrophy of the small muscles of the foot is common in diabetes and is related to peripheral motor neuropathy (1). The atrophy is believed to be the main factor responsible for the development of an imbalance between the flexor and extensor muscles, which results in clawing of the toes, prominent metatarsal heads, and the development of high foot pressures that play a direct role in the development of foot ulceration (2). Currently, there are no established methods to evaluate and follow the progress of small muscle atrophy in diabetic patients. As a result, little information is available regarding the onset of muscle changes and the natural history of their progression in diabetes.

Concentrations of phosphorus-31 ($^{31}$P) cellular metabolites in skeletal muscle change immediately with the onset of ischemia and return quickly to normal levels in viable muscle tissue after reperfusion (3,4). Thus a method that accurately quantifies $^{31}$P metabolite concentrations in foot muscles in vivo and spatially maps the resulting values to an anatomic, radiological image of the foot would be a sensitive, direct indicator of the health of muscle tissue in the diabetic foot. Magnetic resonance imaging (MRI) and magnetic resonance spectroscopy (MRS) provide data for the noninvasive assessment of deep-lying soft tissue anatomy (5–7). Recent studies performed at our facility and elsewhere have demonstrated that the MRI pulse sequence known as rapid acquisition with relaxation enhancement (RARE), which was developed for $^{1}$H MRI, can be modified to directly acquire images of human skeletal muscle and myocardium that spatially map $^{31}$P metabolites; this method provides improved temporal and spatial resolution over that obtained through $^{31}$P MRS methods (8–11).

In the present study, we used the RARE MRI method to acquire $^{31}$P images of the forefeet of neuropathic diabetic patients, nonneuropathic diabetic patients, and healthy control subjects. The main aims of the study were to characterize changes in the foot small muscles and correlate them with clinical measurements of diabetic neuropathy.

## RESEARCH DESIGN AND METHODS

— The study cohort included 12 neuropathic diabetic, 9 nonneuropathic diabetic, and 12 healthy

From the [1]Department of Radiology, Beth Israel Deaconess Medical Center, Harvard Medical School, Boston, Massachusetts; the [2]Department of Medicine, Beth Israel Deaconess Medical Center, Harvard Medical School, Boston, Massachusetts; and the [3]Joslin-Beth Israel Deaconess Foot Center and Microcirculation Laboratory, Beth Israel Deaconess Medical Center, Harvard Medical School, Boston, Massachusetts.

Address correspondence and reprint requests to Robert L. Greenman, PhD, Department of Radiology, Beth Israel Deaconess Medical Center, 330 Brookline Rd., Boston, MA 02115. E-mail: rgreenma@bidmc.harvard.edu.

Received for publication 11 January 2005 and accepted in revised form 21 February 2005.

**Abbreviations:** ABI, ankle brachial index; FOV, field of view; MRI, magnetic resonance imaging; MRS, magnetic resonance spectroscopy; NDS, Neuropathy Disability Score; RARE, rapid acquisition with relaxation enhancement; SWM, Semmes-Weinstein monofilaments; VPT, vibration perception threshold.

A table elsewhere in this issue shows conventional and Système International (SI) units and conversion factors for many substances.

nondiabetic subjects. A diagnosis of type 1 or type 2 diabetes was established according to the recommendations of the American Diabetes Association (12). Subjects with open lesions on their feet, peripheral vascular disease (symptoms of claudication and absence of peripheral pulses, ankle brachial index [ABI] < 0.7]), any other serious chronic diseases requiring active treatment, or a contraindication to MRI examination were excluded from the study. The study protocol was approved by the Institutional Review Board of Beth Israel Deaconess Medical Center and all participants gave written informed consent.

Patients' medical history, including history of alcohol consumption, type and duration of diabetes, and the presence of other micro- or macrovascular complications, was obtained. Patient characteristics, including age, sex, weight, height, and BMI were also evaluated.

### Neuropathy evaluation

The presence of diabetic peripheral neuropathy was defined according to the principles of the San Antonio Consensus criteria (13). For this, the Neuropathy Symptom Score and the Neuropathy Disability Score (NDS) were evaluated as previously described (14). The vibration perception threshold (VPT) was evaluated using a biothesiometer (Biomedical Instruments, Newbury, OH). The cutaneous pressure perception threshold was evaluated using a set of eight Semmes-Weinstein monofilaments that apply a 1- to 100-g pressure. Details of these techniques have been described elsewhere (14). Neuropathy was diagnosed when two or more measurements were abnormal.

### Magnetic resonance imaging data acquisition

$^{31}$P RARE and $^{1}$H MRI were performed on all study subjects using a whole-body 3.0T MR Scanner (General Electric Medical Systems, Milwaukee, WI). A "birdcage" radio frequency coil designed specifically to acquire both $^{31}$P and $^{1}$H MRI data (15,16) was constructed at our facility. Thus $^{31}$P and high-resolution $^{1}$H registration images could be acquired without moving the subject's foot, which resulted in improved registration of the $^{31}$P and $^{1}$H images. A reference standard containing an aqueous solution of 220 mmol/l inorganic phosphate was rigidly attached to the radio frequency coil. The standard was present during all MRI procedures and served two purposes: *1*) the measurement of the $^{31}$P concentration and *2*) as a fiduciary marker for the coregistration of $^{31}$P and $^{1}$H images. All of the acquisitions were performed in the axial plane. The subjects were placed on the scanning bed in the supine position with their knees elevated ~30 cm using a foam cushion. One foot was placed into the birdcage radio frequency coil so that the metatarsal heads were at the center of the coil.

To acquire detailed images of the foot anatomy and delineate regions of edema, fatty infiltration, and scar tissue, T2-weighted $^{1}$H spin-echo imaging was first performed on all subjects (repetition time [TR] = 1.5 s, echo time [TE] = 30 ms, field of view [FOV] = 15 cm, matrix = 256 × 256, slice thickness = 2.5 mm, scan time = 6 min 24 s). Images oriented in the axial plane were acquired at each of 10 contiguous locations. The 10 slice locations of the $^{1}$H acquisition were prescribed so that the maximum extent of coverage in the axial direction was identical to that of the single-slice $^{31}$P RARE image acquisition, described below.

Axial $^{31}$P image data were acquired using the RARE pulse sequence (two echo trains, 32 echoes per echo train, receiver bandwidth = 4 kHz, TR = 12 s, FOV = 30 cm, matrix = 64 × 64, slice thickness = 25 mm, 10 signal averages, scan time = 4 min, voxel volume = 0.55 $cm^3$). In the RARE pulse sequence, the time spacing between the echoes can be adjusted to facilitate constructive or destructive interference of the three ATP resonances (10,17). The echo spacing and effective TE were selected to maximize the destructive interference of the ATP resonances. This substantially suppressed the ATP contribution to the $^{31}$P images. The resulting image intensities were proportional to the combined concentrations of the inorganic phosphate and phosphocreatine cellular metabolites.

### Data processing

Image data were analyzed using Interactive Data Language software (Research Systems, Boulder, CO). The background noise of each $^{31}$P image was measured and a threshold technique was used to eliminate it, leaving only the $^{31}$P signal from muscle and the reference standard. An outline of the muscle tissue and the reference standard was created using a contour mapping function set to a single level that was equal to the noise threshold value. The $^{31}$P muscle outline was registered to one of the central $^{1}$H T2-weighted images, using the reference standard as a fiduciary marker. The average $^{31}$P concentration values were measured and calculated using the $^{31}$P reference standard and a previously described method (10).

The in-plane area across the entire axial view of the foot was calculated for each subject. The 10 $^{1}$H T2-weighted images were added together to create a single image that represented the range covered by the $^{31}$P imaging. The in-plane (cross-sectional) area of each pixel was calculated from knowledge of the image FOV and the number of pixels in the image (matrix size). The pixels that represented a signal from the foot tissues were then counted and the resulting number was multiplied by the pixel size. The cross-sectional area of the muscle tissue was calculated by counting the number of pixels in the $^{31}$P images in the same manner.

### Statistical analysis

The Minitab statistical package (Minitab, State College, PA) for personal computers was used for statistical analysis. The ANOVA test, followed by the Fisher's test, was used to identify differences among the various groups. Correlation between variables was tested using Pearson correlation analysis. All of the tests were two-tailed with $\alpha = 0.05$. Data are presented as means ± SD.

**RESULTS** — The clinical characteristics of the study groups are shown in Table 1. A history of foot ulceration was present in five (50%) of the neuropathic diabetic patients, and in none of the participants in the other two groups. No ulcers were present in any participant at the time of the study.

The $^{31}$P and $^{1}$H MRI images obtained using the 3.0T whole-body MR scanner from a healthy, nondiabetic subject and a nonneuropathic diabetic patient are shown in Fig. 1. As described in the figure legend, despite the fact that no clinical neuropathy was present, changes can be clearly seen in both the $^{31}$P and the $^{1}$H MRI images that were acquired from the diabetic patient, indicating that these changes preceded the development of clinical neuropathy.

The results of the muscle area–to–

**Table 1—*Characteristics of the study population***

| | Control | Nonneuropathic | Neuropathic |
|---|---|---|---|
| *n* | 12 | 9 | 10 |
| Age (years) | 52 ± 14 | 56 ± 8 | 51 ± 7 |
| Sex (male/female) | 8/4 | 6/3 | 8/2 |
| BMI (kg/m$^2$) | 29.6 ± 6.9 | 32.0 ± 6.0 | 33.0 ± 4.7 |
| Diabetes type (1/2) | — | 0/7 | 2/8 |
| Diabetes duration (years)* | — | 6 ± 6 | 23 ± 12 |
| Ankle brachial index† | 1.1 ± 0.1 | 1.1 ± 0.1 | 0.9 ± 0.2 |
| Neuropathy Symptom Score† | 0 ± 0 | 2 ± 2 | 4 ± 2 |
| NDS‡ | 0 ± 0 | 2 ± 1 | 13 ± 8 |
| VPT‡ | 8 ± 3 | 13 ± 6 | 37 ± 16 |
| SWM‡ | 3.88 ± 0.36 | 4.08 ± 0.54 | 6.16 ± 0.77 |

Data are means ± SD. *$P < 0.01$ for nonneuropathic vs. neuropathic; †$P < 0.01$ for control and nonneuropathic vs. neuropathic; ‡$P < 0.0001$ for control and nonneuropathic vs. neuropathic.

total area ratio calculation differed among all three groups: 0.55 ± 0.04 vs. 0.44 ± 0.05 vs. 0.06 ± 0.06 for the control, nonneuropathic, and neuropathic groups, respectively ($P < 0.0001$) (Fig. 2*A*). Average $^{31}$P concentrations also differed among the three groups: 27.7 ± 3.8 vs. 21.7 ± 4.8 vs. 7.9 ± 8.8 mmol/l for the control, nonneuropathic, and neuropathic groups ($P < 0.0001$) (Fig. 2*A*). No differences were observed between the measurements in male and female subjects (data not shown).

When all subjects were considered as one group, the muscle area−to−total area ratios strongly correlated with clinical measurements of the severity of neuropathy, including the NDS ($r = -0.83$, $P < 0.0001$) (Fig. 3), VPT ($r = -0.79$,

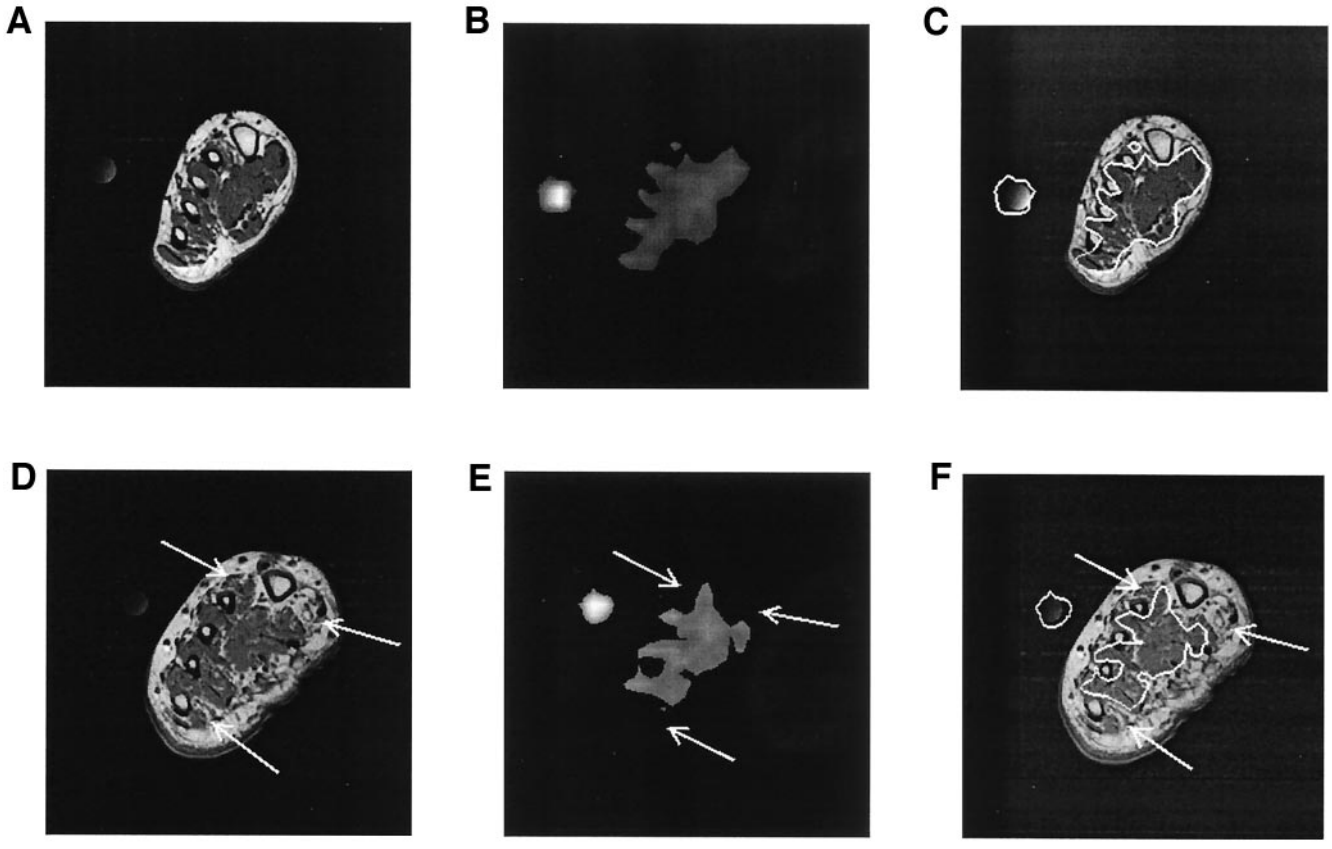


**Figure 1—***$^{31}$P and $^{1}$H MRI results of a normal control subject* (A, B, *and* C) *and a nonneuropathic diabetic patient* (D, E, *and* F). A *and* D *are $^{1}$H T2-weighted MR images that provide anatomical information, whereas* B *and* E *are $^{31}$P images.* C *and* F *show the registration of the outline of the $^{31}$P images onto the $^{1}$H T2-weighted images. The circular object to the left of the foot in the images is the $^{31}$P reference standard, which was also used as a fiduciary marker to aid in the registration of the $^{31}$P outline to the $^{1}$H image. Muscle is the only tissue of the foot with enough $^{31}$P concentration to be detectable by MRI. Thus, the $^{31}$P images* (B *and* E) *represent only the muscle tissue and the $^{31}$P reference standard. Fat, bone, and connective tissue do not appear in the $^{31}$P images. The nonneuropathic subject* (D, E, *and* F) *had NDS, VPT, and SWM values of 2, 20, and 3.22, respectively. Although this subject was nonneuropathic, structural changes are clear in the $^{1}$H T2-weighted image* (D), *where focal regions of fatty infiltration are visible near the large and small toes (arrows). The $^{31}$P concentration is absent in the regions of the $^{31}$P image (arrows in* E) *that correspond to the regions of fatty infiltration in $^{1}$H image. The average $^{31}$P concentration across the entire muscle area calculated from the signal intensity of the normal subject* (B) *was 28.2 mmol/l and of the nonneuropathic diabetic subject was 21.5 mmol/l. The total area−to−muscle area ratio of the normal subject was 0.56 and that of the nonneuropathic diabetic subject was 0.44. The $^{31}$P/$^{1}$H registration image* (F) *shows the correspondence between the regions of undetectable $^{31}$P concentration in* E *and the regions of fatty infiltration in the $^{1}$H image of* D.

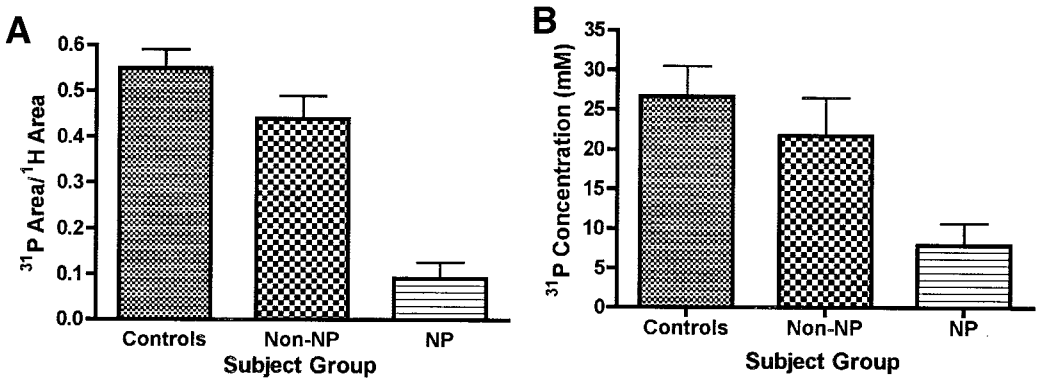


**Figure 2**—*The ratio of muscle cross-sectional area to total cross-sectional area* (A) *and the mean $^{31}$P concentration* (B) *across the metatarsal head region of healthy control, nonneuropathic diabetic (non-NP), and neuropathic (NP) subjects. Significant differences in the cross-sectional area ratios existed among all three groups, with the mean area being higher in the control group and lower in the neuropathic group* ($P < 0.0001$). *The mean $^{31}$P concentration was also significantly different among all three groups* ($P < 0.0001$).

$P < 0.0001$), and SWM ($r = -0.87$, $P < 0.0001$) scores. It also correlated with diabetes duration ($r = -0.56$, $P < 0.05$) and ABI ($r = 0.75$, $P < 0.0001$), whereas no correlations were observed with age or BMI. Multivariate regression analysis showed that only NDS was an independent factor.

The $^{31}$P concentration also correlated with the NDS ($r = -0.73$, $P < 0.001$), VPT ($r = -0.69$, $P < 0.05$), SWM ($r = -0.75$, $P < 0.01$), and ABI ($r = 0.73$, $P < 0.001$) scores. Multivariate regression analysis showed that only SWM was an independent factor.

**CONCLUSIONS** — In the present study, $^{31}$P RARE and $^{1}$H T2-weighted spin-echo MRI were performed on the feet of neuropathic and nonneuropathic patients and normal control subjects. A reduced ratio of viable muscle tissue to all other types of tissue was observed in the feet of both nonneuropathic and neuropathic diabetic patients as compared with normal control subjects. Similarly, a reduction in the average $^{31}$P concentration in both the nonneuropathic and neuropathic diabetic patients was observed when compared with the healthy, nondiabetic control subjects. Furthermore, the observed changes strongly correlated with clinical measurements of peripheral nerve function, indicating an association between muscle atrophy and diabetic neuropathy. Our results indicate that muscle changes in the diabetic foot begin during the subclinical stage of diabetic neuropathy and before the development of clinical signs of the disease.

Small muscle atrophy is a well-known process in the diabetic foot and is related to the development of diabetic motor neuropathy. However, given the paucity of techniques that can quantify muscle atrophy, these changes have not been adequately studied. Instead, motor neuropathy has been evaluated mainly by measuring the motor peroneal conduction velocity and sensory neuropathy has been evaluated through quantitative sensory testing (18). Because small muscle atrophy is the main process that leads to anatomical foot changes, such as clawing

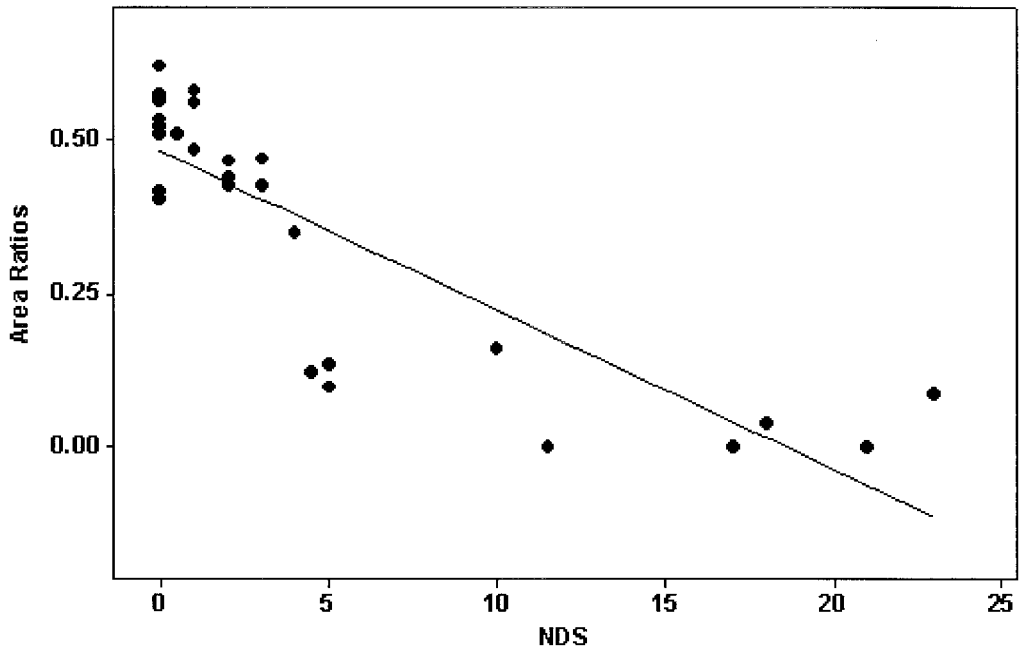


**Figure 3**—*Plot of the ratio of muscle area to total area against the NDS. A strong correlation was observed when all subjects were considered as one group* ($r = -0.83$, $P < 0.0001$).

of the toes and prominent metatarsal heads, that are directly related to the development of foot ulceration, the direct evaluation of muscle changes rather than nerve function may prove more helpful in clinical research studies. More specifically, evaluating changes in the ratio of viable muscle tissue to all other types of foot tissues using $^{1}$H MRI and images based on the $^{31}$P cellular metabolite activity of muscle potentially allows clinicians to detect anatomic and metabolic changes and relate these changes to the development of foot ulceration and wound healing potential.

All previously published studies of $^{1}$H MRI have agreed about the existence of small muscle atrophy in neuropathic diabetic patients (6,7,19,20). However, there have been no reports of atrophy in nonneuropathic patients. We believe that the difference between our results and those of previous studies is related to the specific techniques used. Previous studies have used T1-weighted (20) or T2-weighted imaging methods (6) and T2 mapping techniques (6) to evaluate the cross-sectional area of muscle tissue. However, as muscle atrophy occurs, the T1 and T2 relaxation rates in muscle-containing regions increase, causing the various tissue types to become nearly isointense with each other. This obscures the tissue boundaries, thus making it difficult or impossible to segment or determine the threshold of muscle tissue from adjacent tissues, as acknowledged by the authors of one study (6). In contrast to segmentation and thresholding methods, the distinction between muscle tissue and other tissues in the foot using $^{31}$P RARE MRI is straight forward because muscle is the only tissue of the foot that has $^{31}$P concentrations that are detectable by MRI. Therefore, the $^{31}$P RARE MRI method offers a more accurate evaluation of viable muscle tissue; in our study, this method allowed us to identify relatively small changes in the nonneuropathic patients in comparison with the status of healthy nondiabetic subjects.

In a recently published study, Andersen et al. (20) calculated the total volume of foot muscles from $^{1}$H MRI by segmenting the muscle tissue using an image-intensity threshold method. Although the total muscle volume was significantly reduced in neuropathic diabetic patients compared with in control subjects, no difference was found between the nonneuropathic diabetic patients and control subjects. Because the total muscle volume is related to the foot size, the results of the Andersen et al. study (20) may have been influenced by differences in foot size among the various groups. In the present study, we compared the ratio of the cross-sectional muscle area to the total cross-sectional area at the same location in the foot; this ratio gave us a better indication of the amount of muscle loss by eliminating differences in foot size among population groups. In addition, we used $^{31}$P RARE MRI, which provided a direct measurement of the amount of muscle tissue. This different methodology resulted in a sensitive technique that enabled us to more accurately detect differences in muscle atrophy among various groups. We believe that this was the main reason for the observed differences between our results and the results of the previous study.

MRS was used in one previous study that examined changes between diabetic patients and healthy control subjects (5). The results of that study demonstrated changes in the $^{31}$P metabolites and an increased fat-to-water ratio in diabetic patients with superficial ulcers compared with diabetic patients without ulcers and healthy subjects, whereas no differences were observed between diabetic patients without foot ulceration and healthy control subjects. As with the previous studies, we believe that the differences between our findings and the results of the MRS study are related to the techniques used. The $^{31}$P MRS method used in the previous study (5) resulted in $^{31}$P data sets with a spatial resolution of 11.25 cm$^3$ (requiring a scan time of >50 min), whereas in the present study the $^{31}$P images had a spatial resolution of 0.55 cm$^3$ (requiring a scan time of 4 min). The improved spatial resolution of the $^{31}$P RARE method resulted in better identification of focal regions of reduced $^{31}$P concentration when compared with the previous MRS methods. In addition, the higher spatial resolution of the $^{31}$P RARE MRI method allowed a more accurate delineation of the boundaries and contours of the muscle tissue, thus providing better registration with $^{1}$H anatomical images and a more accurate measurement of the muscle cross-sectional area.

The concentration of various $^{31}$P metabolites is also influenced by the presence of ischemia. Thus, when muscle is ischemic, the concentration of phosphocreatine decreases from its normal value as the concentration of inorganic phosphate increases (3,4). Preliminary ongoing studies at our facility indicate that the grading of the degree of ischemia is feasible and can be achieved using $^{31}$P RARE MRI to create separate phosphocreatine and inorganic phosphate images in the diabetic foot. However, in the present study we used $^{31}$P RARE MRI to acquire data that reflected the combined concentrations of phosphocreatine and inorganic phosphate, as we aimed to identify metabolically active muscle tissue and not to grade the degree of muscle ischemia.

In the present study, in agreement with previous studies, we observed strong correlations between quantitative clinical measurements of the severity of neuropathy and the muscle area−to−total area ratio or $^{31}$P measurements (5,20). In addition, strong correlations were observed between the muscle area−to−total area ratio or $^{31}$P concentration measurements and the duration of diabetes and the ABI. However, as the multiple regression analysis excluded these parameters as independent factors, it can be concluded that the severity of neuropathy was the only factor that influenced these measurements. Finally, there were no differences between male and female subjects in the muscle area−to−total area ratio or $^{31}$P measurements, and no correlations were noticed between BMI and the above measurements. These findings further indicate that the size of the foot did not influence the observed results.

A word of caution should be added at this point. The term "nonneuropathic diabetic patient" indicates a patient in whom there is no evidence of clinical neuropathy as determined using standard, widely used clinical techniques. However, the existence of subclinical neuropathy in these patients cannot be excluded. Because previous studies using sophisticated experimental techniques have shown subclinical nerve function abnormalities in most diabetic patients, it seems reasonable to suspect that such changes were also present in the nonneuropathic patients who participated in this study. Despite this, we believe that the results of our study are still interesting and the conclusions are still valid, as they indicate that changes in foot muscles occur before changes in nerve function can be detected

using standard techniques available to the practicing clinician.

In summary, we have shown that small muscle atrophy is present in diabetes before clinical peripheral neuropathy can be detected using standard techniques available in clinical practice. The $^{31}$P RARE MRI method can evaluate the severity of muscle atrophy, even in the early stages when clinically detectable neuropathy is absent. Furthermore, the muscle tissue in patients can be noninvasively evaluated within a short time using this MRI method compared with existing localized MRS methods. The $^{31}$P RARE MRI method may prove to be a useful diagnostic tool that can facilitate the implementation of clinical trials in the early stages of diabetic foot problems as well as monitor the response to treatment.

**Acknowledgments**— The study was supported in part by research grants from the Juvenile Diabetes Research Foundation International (JDRF 5-2002-329) and the National Institutes of Health (R01-HL0-75678-01 to A.V., R21-DK-58651 to R.L.G., and RR-01032 to the Beth Israel Deaconess Medical Center General Clinical Research Center).

**References**

1. Boulton A: 18th Camillo Golgi Lecture. The diabetic foot: from art to science. *Diabetologia* 47:1343–1353, 2004
2. Caselli A, Pham H, Giurini J, Armstrong D, Veves A: The forefoot-to-rearfoot plantar pressure ratio is increased in severe diabetic neuropathy and can predict foot ulceration. *Diabetes Care* 25:1066–1071, 2002
3. Hands L, Bore P, Galloway G, Morris P, Radda G: Muscle metabolism in patients with peripheral vascular disease investigated by 31P nuclear magnetic resonance spectroscopy. *Clin Sci* 71:283–290, 1986
4. Martin P, Gibson H, Edwards R: MRS of muscle. In *MR Spectroscopy*: *Clinical Applications and Techniques*. Young I, Charles H, Eds. London, Martin Dunitz, 1996, p. 55–73
5. Suzuki E, Kashiwag A, Hidaka H, Maegawa H, Nishio Y, Kojima H, Haneda M, Yasuda H, Morikawa S, Inubushi T, Kikkawa R: 1H and 31P-magnetic resonance spectroscopy and imaging as a new diagnostic tool to evaluate neuropathic foot ulcers in type II diabetes. *Diabetologia* 43:165–172, 2000
6. Bus SA, Yang QX, Wang JH, Smith MB, Wunderlich R, Cavanagh PR: Intrinsic muscle atrophy and toe deformity in the diabetic neuropathic foot: a magnetic resonance imaging study. *Diabetes Care* 25: 1444–1450, 2002
7. Brash P, Fostert J, Vennart W, Anthony P, Tooke J: Magnetic resonance imaging techniques demonstrate soft tissue damage in the diabetic foot. *Diabet Med* 16: 55–61, 1999
8. Greenman RL, Elliott MA, Vandenborne K, Schnall MD, Lenkinski RE: Fast imaging of phosphocreatine using a RARE pulse sequence. *Magn Reson Med* 39:851–854, 1998
9. Greenman RL, Axel L, Ferrari VA, Lenkinski RE: Fast imaging of phosphocreatine in the normal human myocardium using a three-dimensional RARE pulse sequence at 4 Tesla. *J Magn Reson Imaging* 15:467–472, 2002
10. Greenman RL: Quantification of the 31P metabolite concentration in human skeletal muscle from RARE signal intensity. *Magn Reson Med* 52:1036–1042, 2004
11. Chao H, Bowers JL, Holtzman D, Mulkern RV: RARE imaging of PCr in human forearm muscles. *J Magn Reson Imaging* 7:1048–1055, 1997
12. Report of the Expert Committee on the Diagnosis and Classification of Diabetes Mellitus. *Diabetes Care* 20:1183–1197, 1997
13. Report and Recommendations of the San Antonio Conference on Diabetic Neuropathy. Consensus Statement. *Diabetes* 37: 1000–1004, 1988
14. Pham H, Armstrong DG, Harvey C, Harkless LB, Giurini JM, Veves A: Screening techniques to identify people at high risk for diabetic foot ulceration: a prospective multicenter trial. *Diabetes Care* 23:606–611, 2000
15. Hayes CE, Edelstein WA, Schenck JF, Mueller OM, Eash M: An efficient, highly homogeneous radiofrequency coil for whole-body NMR imaging at 1.5 T. *J Magn Reson* 63:622–628, 1985
16. Isaac G, Schnall M, Lenkinski R, Vogele K: A design for a double-tuned birdcage coil for use in an integrated MRI/MRS examination. *J Magn Reson* 89:41–50, 1990
17. Chao MS, Bowers JL, Holtzman D, Mulkern RV: Multi-echo 31P spectroscopic imaging of ATP: a scan time reduction strategy. *J Magn Reson Imaging* 7:425–433, 1997
18. Veves A: Diagnosis of diabetic neuropathy. In *The Clinical Management of Diabetic Neuropathy*. Veves A, Ed. Totowa, NJ, Humana, 1998, p. 61–75
19. Andersen H, Gadeberg P, Brock B, Jakobsen J: Muscular atrophy in diabetic neuropathy: a stereological magnetic resonance imaging study. *Diabetologia* 40: 1062–1069, 1997
20. Andersen H, Gjerstad M, Jakobsen J: Atrophy of foot muscles: a measure of diabetic neuropathy. *Diabetes Care* 27:2382–2385, 2004